Catalysis Today 167 (2011) 84–90

Contents lists available at ScienceDirect

Catalysis Today

journal homepage: www.elsevier.com/locate/cattod

Etherification of glycerol to polyglycerols over MgAl mixed oxides

Cristina García-Sancho, Ramón Moreno-Tost, Josefa M. Mérida-Robles, José Santamaría-González, Antonio Jiménez-López, Pedro Maireles Torres*

Dpto. Química Inorgánica, Cristalografía y Mineralogía (Unidad Asociada al ICP-CSIC), Campus de Teatinos s/n, 29071 Málaga, Spain

ARTICLE INFO

Article history:
Received 14 June 2010
Received in revised form 8 October 2010
Accepted 5 November 2010
Available online 22 December 2010

Keywords:
Hydrotalcite
Polyglycerol
Glycerol
MgAl mixed oxides

ABSTRACT

This work investigates the use of MgAl mixed oxides as base catalysts for the etherification of glycerol. Two different experimental strategies have been employed for the synthesis of the hydrotalcite precursors: coprecipitation and urea hydrolysis. The hydrotalcites and catalysts were characterized by X-ray diffraction, X-ray photoelectron spectroscopy, scanning electron microscopy, CO_2-temperature programmed desorption and N_2 adsorption. The MgAl mixed oxides exhibit excellent textural properties, with specific surface areas higher than 200 $m^2\,g^{-1}$ and average pore diameters in the mesoporous range. This series of catalysts have shown to be active in the formation of polyglycerols from glycerol without solvent, at 220 °C, in a batch reactor. The highest conversion (50.7%) is found for the catalyst prepared by coprecipitation using $NaOH/Na_2CO_3$ as precipitating agent, whereas full selectivity to diglycerols is only reached for low conversion values (14.6% for sample prepared by urea hydrolysis). Only diglycerols (DGs) and triglycerols (TGs) have been detected after 24 h of reaction, with a maximum DG yield of 43% with the catalysts having the highest specific surface area. The formation of DG is favored at low conversion and in the presence of small pores.

1. Introduction

Currently, biodiesel production is mainly based on the transesterification of the triglycerides of vegetable oils and animal fats with methanol, in the presence of an acid or base catalyst. Each triglyceride molecule gives rise to three molecules of fatty acid methyl (ethyl) esters (FAME or FAEE) and a molecule of glycerol (1,2,3-propanetriol). Due to biodiesel is industrially produced worldwide, the production of glycerol has notably increased causing as consequence a drop in its price. In this way, the glycerol has been turned into an interesting starting raw material for other value-added chemicals. Thus, the glycerol could be transformed into valuable fine chemicals, thus improving the economic viability of a biodiesel plant and therefore, transforming the current biodiesel industry into a biorefinery based on the oleochemical platform. Up to the growing biodiesel production, glycerol was mainly obtained in four different processes: soap manufacture, fatty acid production, fatty ester production and microbial fermentation as well as from propylene oxide [1]. Glycerol itself has many applications such as in pharmaceuticals, cosmetics, soaps and toothpastes, sweetener and as a wetting agent in tobacco [2]. As glycerol is a highly functionalized molecule, large number of valuable chemicals can be obtained by a variety of chemical reactions including, in all of them, the heterogeneous catalysis as a key step [3]. Hence, intense research in science and industry field has been made to valorise this surplus of glycerol. In literature, several catalytic reactions have been investigated for conversion of glycerol such as hydrogenolysis to yield propanediols [4–6], conversion to synthesis gas [7,8], etherification with alkenes [9–11], polymerisation to oligoglycerols [12–14], oxidation [15,16], dehydration to acrolein [17–20] and synthesis of fatty esters [21].

As it has been stated above, the polymerisation of glycerol leads to interesting products which are already utilised in cosmetics and additives in nutrition or lubricants. The condensation of two glycerol molecules yields the simplest polyglycerol, called diglycerol and it can be linear, branched or cyclic depending on if the condensation takes place between primary or secondary hydroxyls or an intramolecular condensation is involved [22]. On the other hand, the condensation of glycerol can progress yielding tri-, tetra- and higher polyglycerols. These polyglycerols can be produced with basic homogeneous catalysis like alkali carbonates or hydroxides, the carbonates being more active than hydroxides, in spite of their lower basicity, due to the higher solubility in the glycerol. Acidic catalysts are also active in the condensation of glycerol but acrolein is formed as by-product. However, in the last years, the catalytic studies are being directed toward heterogeneous catalysis. Although heterogeneous catalysts are less active, they exhibit some advantages (i) the catalysts can easily be separated from the reaction mixture, (ii) they can be reused and (iii) theoretically the reaction path can be conducted to a selected product of conden-

* Corresponding author. Tel.: +34 952131873; fax: +34 952137534.
E-mail address: maireles@uma.es (P.M. Torres).

0920-5861/$ – see front matter © 2010 Elsevier B.V. All rights reserved.
doi:10.1016/j.cattod.2010.11.062

sation. An extensive study has been conducted by the Barrault group [12,23–25]. They studied the catalytic behaviour of zeolitic and mesoporous catalysts exchanged or impregnated with alkaline metals.

Concerning the catalytic process of etherification of glycerol, shape-selectivity to di- and tri-glycerol (DG and TG, respectively) has previously been observed at 260 °C when mesoporous MCM-41 silica was used as support of alkaline or alkaline-earth metals, whereas in the case of exchanged and impregnated zeolites the reaction mainly occurred at the external surface due to the reduced pore size of this microporous support, with a low selectivity to DG [24]. By comparing different catalysts, Clacens et al. [25] have found that an increase of the glycerol conversion leads to a loss of selectivity, lowering the selectivity to DG and increasing that of TG. The best results were obtained with caesium-based mesoporous catalysts, although significant leaching of the active species was detected. Moreover, lanthanum- and magnesium-containing mesoporous catalysts favored the glycerol dehydration to acrolein.

On the other hand, Ruppert et al. [26] studied alkaline-earth metal oxides in this reaction at a lower temperature (220 °C) and compared the catalytic results with homogeneous Na_2CO_3. It was found that glycerol conversion increased with increasing catalyst basicity: MgO < CaO < SrO < BaO. The best selectivity values for (di- + tri-) glycerol (>90% at 60% conversion) were obtained over CaO, SrO, and BaO, with no substantial acrolein formation. However, alkaline earth oxides suffer from instability toward ambient water and carbon dioxide, giving rise to less basic species and requiring very high activation temperatures.

Basic metal oxides derived from layered double hydroxides (LDHs) have been extensively studied due to their tunable properties that have allowed them to find potential applications in different catalytic fields [26–29]. Most LDHs adhere to the general chemical formula: $[M^{II}_{1-x}M^{III}_{x}(OH)_2]^{x+}-(A^{n-})_{x/n}\cdot 3H_2O$, where M^{II} represents any divalent metal cation, M^{III} any trivalent metal cation, and A^{n-} an anion (inorganic or organic). The thermal decomposition of MgAl-hydrotalcites leads to a high-surface-area $Mg(Al)O_x$ mixed oxide with strong O^{2-} Lewis basic sites [30]. These structural modifications are accompanied by an increase in specific surface area. The acid–base properties and, as a consequence, the catalytic activity and selectivity of these MgAl-mixed oxides depend on chemical composition and on the conditions of the thermal treatment used to decompose the hydrotalcite precursor. With respect to the chemical composition, the optimum Mg/Al ratio will depend on the basic site density and strength required to activate the particular reactant. In this sense, calcined hydrotalcites exhibit enough strength to be used in the transesterification of triglycerides under heterogeneous conditions [31–34].

The goal of the present work was to evaluate the catalytic behaviour in etherification of glycerol to obtain polyglycerols without solvents of MgAl mixed oxides derived from hydrotalcite. Different synthetic routes have been used in order to study the influence on the structural and textural properties. Hydrotalcite precursors and catalysts have been characterized by X-ray diffraction, XPS, SEM, N_2-adsorption–desorption and CO_2-TPD, with the objective of looking for structure–activity relationships which help us to explain the catalytic behaviour of this family of solids.

2. Experimental

2.1. Catalyst synthesis

The coprecipitation at pH constant and the urea hydrolysis methods have been chosen to synthesize Mg/Al hydrotalcites. The Mg/Al molar ratio was 3 and the total concentration of cations was 1 M. In the coprecipitation method, the synthesis was carried out at room temperature by using the corresponding metal nitrates and the resulting solution was aged during 42 h under vigorous stirring. The pH of the solution was maintained at 10, and it was achieved by using three different precipitant solutions: $NaOH/Na_2CO_3$, KOH/K_2CO_3 and NH_3 aqueous solution/$(NH_4)_2CO_3$ with a molar ratio of 16. In the case of the urea method, the hydrolysis of urea took place at 100 °C in a three round necked-flask equipped with reflux and thermometer. The reaction was allowed to progress during 42 h, being the pH = 7.7 at the end of the synthesis. In all cases, solids were filtered, deeply rinsed with distilled water and dried at 65 °C. The materials were labelled as MgAl_Na, MgAl_K, MgAl_N and MgAl_U. The hydrotalcites were activated in a tubular furnace at 450 °C during 15 h to transform them in the corresponding MgAl mixed oxide.

2.2. Catalyst characterization

Elemental analysis was performed on a PERKIN-ELMER 2400 CHN with a LECO VTF900 pyrolysis oven. Mg, Al, Na and K contents have been determined by ICP-AES by using a Perkin Elmer (model ELAN DRC-e) spectrometer.

Powder XRD patterns were obtained by using a Siemens D5000 automated diffractometer, over a 2θ range with Bragg–Brentano geometry using the Cu Kα radiation and a graphite monochromator.

Scanning electron micrographs (SEMs) were obtained by using a JEOL SM 840. Samples were placed over an aluminium drum and covered with a gold film using a JEOL Ion Sputter JFC 1100.

X-ray photoelectron spectroscopy (XPS) studies were performed with a Physical Electronics PHI 5700 spectrometer equipped with a hemispherical electron analyzer (model 80-365B) and a MgKα (1253.6 eV) X-ray source. High-resolution spectra were recorded at 45° take-off-angle by a concentric hemispherical analyzer operating in the constant pass energy mode at 29.35 eV, using a 720 mm diameter analysis area. Charge referencing was done against adventitious carbon (C 1s at 284.8 eV). The pressure in the analysis chamber was kept lower than 5×10^{-6} Pa. PHI ACCESS ESCA-V6.0 F software package was used for data acquisition and analysis. A Shirley-type background was subtracted from the signals. Recorded spectra were always fitted using Gauss–Lorentz curves in order to determine more accurately the binding energy of the different element core levels.

N_2 adsorption–desorption isotherm at −196 °C was obtained using an ASAP 2020 model of gas adsorption analyzer from Micromeritics, Inc. Prior to N_2 adsorption, the sample was evacuated at 450 °C (heating rate 10 °C min^{-1}) for 18 h. Pore size distributions and pore volume were calculated with the BJH method.

The basicity was studied by temperature-programmed desorption of CO_2. Samples (100 mg) were pretreated under a helium stream at 450 °C for 15 h (2 °C min^{-1}, 100 mL min^{-1}). Then, temperature was decreased until 100 °C, and a flow of pure CO_2 (50 mL min^{-1}) was subsequently introduced into the reactor during 1 h. The CO_2-TPD was carried out between 100 and 800 °C under a helium flow (10 °C min^{-1}, 30 mL min^{-1}), and evolved CO_2 was analyzed by an on-line gas chromatograph (Shimadzu GC-14A) provided with a TCD, after passing an ice-NaCl trap to eliminate any trace of water.

2.3. Catalytic reaction

The catalytic activity of this series of catalysts was evaluated in the etherification of glycerol (Aldrich) at 220 °C in a glass batch reactor, equipped with a water-cooled condenser and a thermometer, under inert atmosphere (N_2) and vigorous stirring. The formed water was eliminated by a Dean–Stark system. Before the reaction, catalysts were activated at different temperatures for

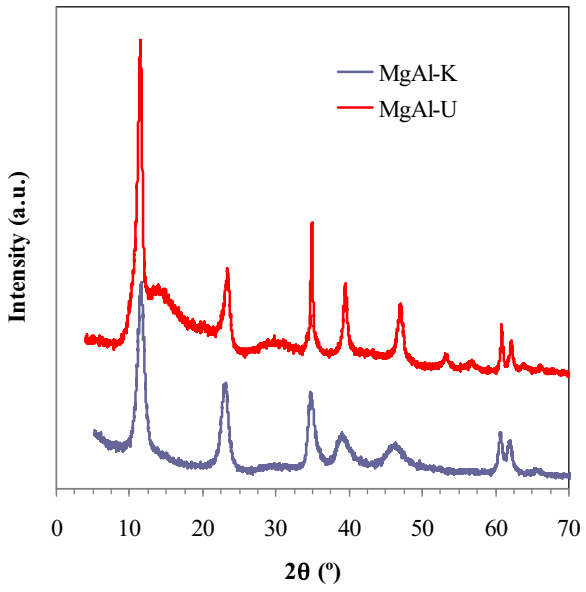

Fig. 1. Powder X-ray diffraction patterns of MgAl_K and MgAl_U hydrotalcites.

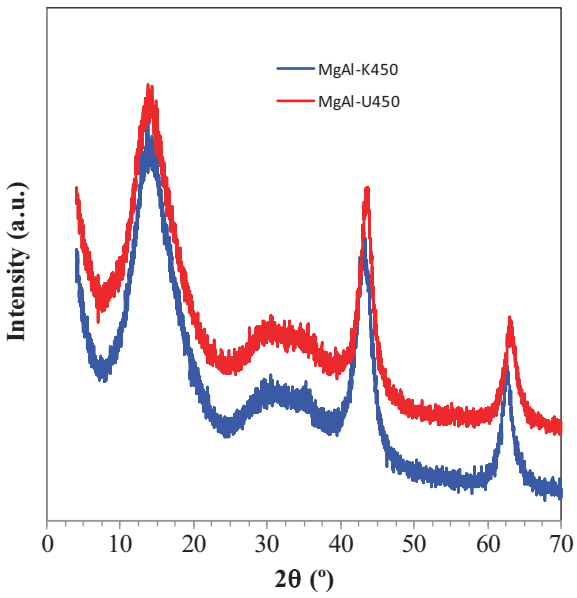

Fig. 2. Powder X-ray diffraction patterns of MgAl_K and MgAl_U samples after activation at 450 °C.

15 h (heating rate, 2 °C min^{-1}) under a helium flow. The reaction was stopped at 24 h and catalysts were separated by filtration. Reaction products were analyzed in a gas chromatograph (Shimadzu GC model 14A) equipped with FID and a capillary silica fused TBR-14 column (Tecknochroma) after silylation with N,O-bis(trimethylsilyl)trifluoroacetamide (Aldrich).

3. Results and discussion

The X-ray diffraction patterns of the as-synthesized hydrotalcites show the presence of the typical diffraction signals associated to the stacked layer ordering of this family of layered double hydroxides (Fig. 1). The lattice parameters *c* and *a* have been calculated from the strongest lines associated to (0 0 3) and (1 1 0) planes, respectively, and the found values (c = 22.6–23.3 Å and a = 3.0–3.1 Å) are very close to those reported by other authors [35,36] for hydrotalcites with carbonates in the interlayer space. The calcination of hydrotalcites at 450 °C leads to the destruction of the layered structure and the formation of a $MgAl(O)_x$ mixed oxide phase with periclase structure (PDF file 087-0653), not evidencing the XRD patterns the presence of remaining hydrotalcite phase (Fig. 2). Moreover, this temperature is in the range in which the corresponding hydroxycarbonates decompose without forming crystalline $MgAl_2O_4$ spinel.

The elemental analysis of the as-synthesised hydrotalcites, prepared by the co-precipitation method (Table 1), shows a good agreement between the composition of metals in the synthesis solution and the Mg/Al molar ratio in the resulting solids, indicating that cations have been successfully incorporated in the hydrotalcite structure. However, the hydrotalcite prepared by the urea method has a Mg/Al molar ratio in the solid lower than that of the initial solution (Table 1). This fact could be related with the lower pH (7.7) of the solution reached after the aging time, lowering the content of magnesium in the structure. The comparison between the bulk and surface Mg/Al molar ratios obtained by ICP-AAS and XPS techniques, respectively, reveals a superficial enrichment of aluminium. The coprecipitation method leads to bulk Mg/Al molar ratios very close to 3, whereas the use of urea as precipitating agent gives rise to a solid with a higher percentage of aluminium (Table 1). This aluminium species could be forming amorphous aluminium hydroxides precipitates, and its presence has been already justified by Adachi-Pagano et al. [37]. This amorphous $Al(OH)_3$ precipitate could be formed under the acid conditions during the earlier step of the synthesis. Similarly, the carbonate content of the MgAl_U hydrotalcite is also lower than the expected value, probably due to the insufficient presence of carbonate ions in the urea solution. Thus, the excess of positive charge of the brucite layer must be compensated by hydroxyl ions. This fact is also confirmed by XRD analysis (Fig. 1) since the XRD pattern of MgAl_U shows the diffraction lines (2θ = 53.3° and 56.7°) characteristics for a sample with hydroxyl ions (OH^-) in the interlayer [37]. It has been previously observed that Al(III) molar fraction in the synthesized hydrotalcite is higher than that in solution, but always lower than 0.44, which is the maximum Al/(Al + Mg) molar ratio for a pure hydrotalcite [38]. The content of alkaline metal (Na, K) was always lower than 0.1 wt%.

Thermal decomposition of hydrotalcite precursors leads to the formation of the corresponding MgAl mixed oxides, whose textural properties depend on the experimental procedure. Thus, a large range of BET surface area and pore volume values can be found in literature. In our case, the calcination at 450 °C gives rise to solids with large specific surface areas, ranging between 240

Table 1
Lattice parameters and chemical analyses of the LDH precursors.

Sample	d_{003} (Å)	c (Å)	a (Å)	%C[a] (CHN)	Bulk Mg/Al molar ratio[b]	Surface Mg/Al molar ratio[c]
MgAl_Na	7.73	23.2	3.1	2.09	3.02	1.23
MgAl_K	7.55	22.6	3.0	2.14	2.86	1.37
MgAl_N	7.68	23.1	3.1	2.05	2.69	1.09
MgAl_U	7.76	23.3	3.0	1.70	1.68	0.97

[a] CHN analysis.
[b] ICP-AAS analysis.
[c] XPS analysis.

Table 2
Textural properties and desorbed CO_2 for the calcined hydrotalcites.

Sample	S_{BET} ($m^2\ g^{-1}$)	Pore volume ($cm^3\ g^{-1}$)	Average pore diameter (nm)	CO_2-TPD[a] ($\mu mol\ CO_2\ g^{-1}$)
MgAl_Na	322	0.975	10.2	68.1
MgAl_K	312	1.088	11.9	54.0
MgAl_N	264	0.687	8.0	52.7
MgAl_U	240	0.265	3.1	56.5

[a] Evolved CO_2 calculated from the first desorption peak.

and 322 $m^2\ g^{-1}$ (Table 2). The best textural properties are obtained when the coprecipitation method is used in the presence of alkaline cations. However, the differences are more important regarding the pore volume values, with values higher than 0.9 $cm^3\ g^{-1}$ for those two samples exhibiting the largest BET surface areas. The smaller values for these textural parameters are observed for the calcined MgAl_U, leading to an average pore diameter close to 3 nm, whereas the mesoporous character of the rest of solids is more pronounced. The N_2 adsorption–desorption isotherms of the MgAl mixed oxides (Fig. 3) are of Type IIb according to the IUPAC classification. The hydrotalcites prepared by the coprecipitation method display a hysteresis loop (Fig. 3), which desorption branch starts immediately after adsorption (H3 hysteresis). This hysteresis loop is characteristic of solids consisting of aggregates of plate-like particles with slit-shaped pores [39,40].

The scanning electron micrographs of hydrotalcite precursors were recorded to study the morphology of the different samples. The SEM images reveal the existence of particles of irregular shapes and without a well-defined shape, being much larger when the urea method is used (Fig. 4). The morphology of the hydrotalcite precursors was maintained after thermal treatment.

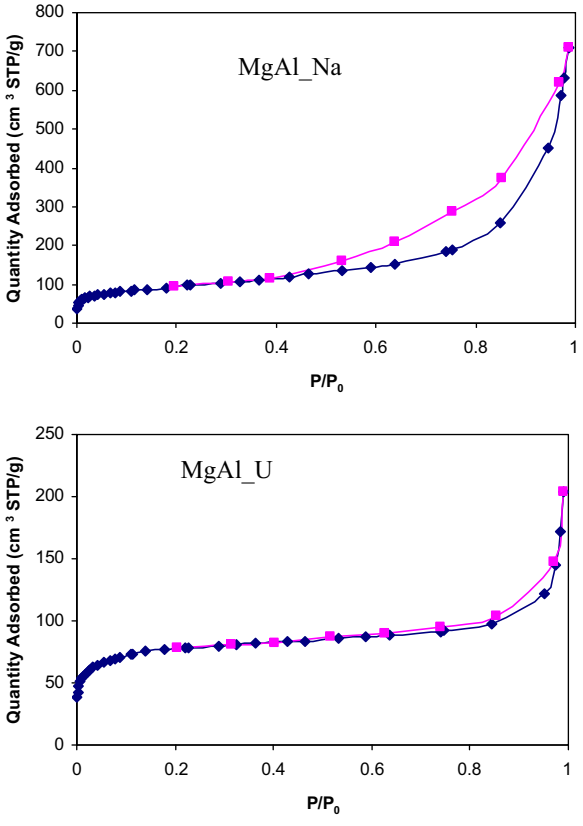

Fig. 3. Nitrogen adsorption–desorption isotherms at −196 °C of MgAl_Na and MgAl_U samples after activation a 450 °C.

The basicity of this family of mixed MgAl oxides has been evaluated by temperature programmed desorption of CO_2 (Fig. 5). This technique affords information about the strength and amount of basic sites from the desorption temperature and the peak area, respectively. In all cases, the graphs exhibit two broad desorption peaks, between 100 and 450 °C and from 500 until 725 °C. The broadening of the low temperature band reflects the presence of basic sites of very different strengths on the surface of these solids, and in all cases two maxima can be observed at values close to 200 and 300 °C. However, the second desorption peak can be attributed to the presence of remaining carbonates due to a residual amorphous $MgCO_3$ phase which is not decomposed at 450 °C, instead of the CO_2 adsorbed on the surface of catalysts during the CO_2-TPD experiment. Moreover, owing to the negligible value of Na and K detected on the pristine hydrotalcites, the evolved CO_2 data displayed in Table 2 can be only associated to the MgAl mixed oxides. The existence of these residual carbonates was confirmed by both FTIR analysis and a CO_2-TPD blank test without adsorbing CO_2 of samples treated at 450 °C, pointing out that carbonates were not totally decomposed at this temperature (results not shown). Thus, the data displayed in Table 2 correspond to the first desorption peak, and indicate that the MgAl_Na catalyst exhibits the highest basicity among this family of catalysts.

Bearing in mind the drawbacks of the etherification of glycerol, such as those associated to the formation of acrolein at high reaction temperature and the leaching of the active phase in the reaction medium, we have decided to employ MgAl mixed oxides derived from hydrotalcites. This family of metal oxides has already demonstrated to have potential applications in many base catalysed organic reactions [41–43].

The etherification reaction of glycerol has been carried out without solvent, by using a batch reactor at 220 °C, at atmospheric pressure under N_2 atmosphere. These catalysts have shown to be active in the etherification of glycerol, showing a different conversion and selectivity depending on the synthesis method of the hydrotalcite precursor. MgAl mixed oxides prepared by using the coprecipitation method gives rise to conversion ranging between 24 and 51%, whereas the use of urea as precipitating agent leads to a lower active mixed oxide, with a conversion of 14.6%. Under these experimental conditions, only DG and TG are observed, as reveals the corresponding chromatograms (Fig. 6). Moreover, the formation of acrolein is not detected.

The highest yield of DG is reached when the calcined MgAl_Na is used, with a percentage of TG close to 15% (Fig. 7). MgAl_U gives rise to a lower glycerol conversion, which could be attributed to the presence of boehmite in this catalyst, as detected by XRD. This low conversion and its smaller pore size lead to a full selectivity to DG.

The etherification of glycerol to yield polyglycerols is shape-selective, as Barrault and co-workers have shown in their experiments with mesoporous solids [12,24,25]. This shape-selectivity is also observed with this MgAl mixed oxides (see Fig. 7). Thus, the most selective catalysts toward the formation of triglycerides were MgAl_K and MgAl_Na, which have the largest pore diameters. On the other hand, the highest selectivity toward diglycerides was found for MgAl_N and MgAl_U, in which the pore diameter size was lower. In this sense, a catalyst could be design

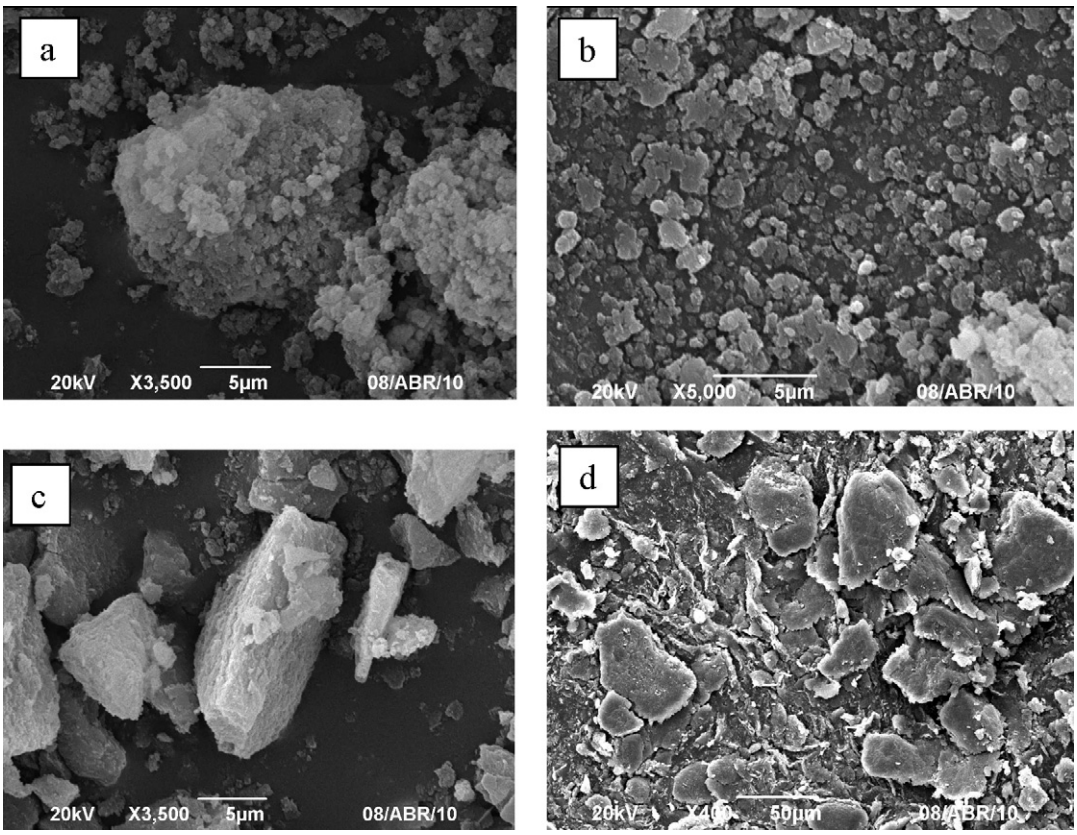

Fig. 4. SEM micrographs of (a) MgAl_Na, (b) MgAl_K, (c) MgAl_N and (d) MgAl_U hydrotalcites.

to yield a determined product by controlling the size of the porous network. However, the catalytic activity is related to the basicity of the catalyst, as measured by CO_2-TPD. As shown in Table 2, a correlation between glycerol conversion and basicity can be also observed, since among the tested catalysts, the MgAl_Na catalyst exhibited the higher catalytic conversion of glycerol besides being the most basic one. However, if a comparison between basicity and activity is made for MgAl_K, MgAl_N and MgAl_U catalysts, the catalytic activity cannot be only explained using the basicity data of the catalysts since the difference of the desorbed CO_2 are minimal. Therefore, for designing a suitable catalyst for the etherification of glycerol, two parameters have to be tuned: the porous network to direct the selectivity to di- or triglycerides and the basicity to achieve an adequate catalytic performance.

The influence of temperature treatment of pristine hydrotalcite was studied with the MgAl_Na sample. In function of DTA–TG analysis (Fig. 8), the hydrotalcite was treated at 200 °C, 450 °C and 650 °C as well as a non-activated. The routine of activation is the same as described in Section 2, heating rate of 2 °C min^{-1} and 15 h at the selected temperature. For the temperatures at 450 °C and 650 °C, the MgAl mixed oxide shows almost full selectivity to DG (Table 3) and at 450 °C is reached the highest glycerol conversion (51%). This

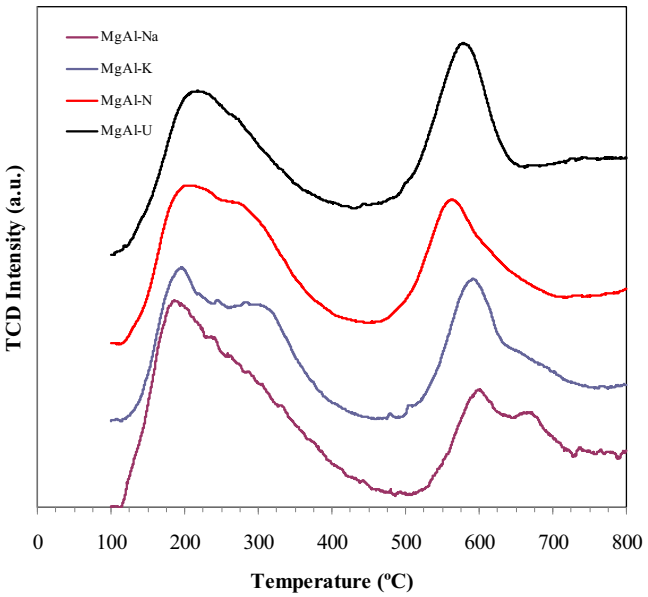

Fig. 5. CO_2 temperature programmed desorption of the MgAl mixed oxides.

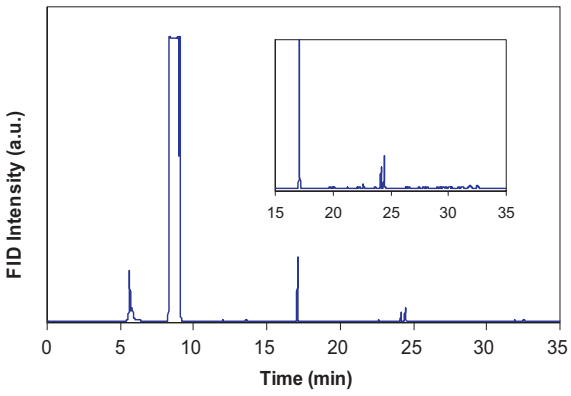

Fig. 6. Typical chromatogram after the etherification process: t < 10 min: pyridine + silylation agent, t = 17.1 min: glycerol, t = 21–24 min: diglycerols and t = 30–32 min: triglycerols.

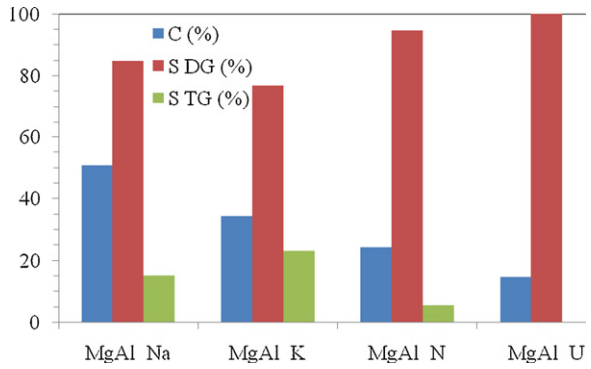

Fig. 7. Glycerol conversion and selectivities to DG and TG in the etherification reaction over the MgAl mixed oxides (reaction conditions: glycerol = 15 g, catalyst weight: 300 mg; temperature: 220 °C, reaction time: 24 h).

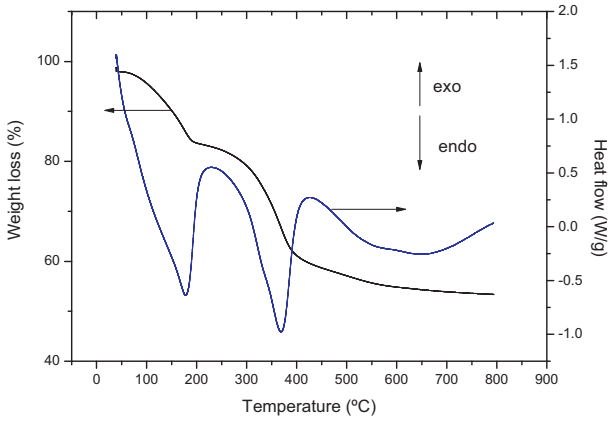

Fig. 8. Thermogravimetric and differential thermal analyses (TG–DTA) of the MgAl_Na hydrotalcite.

fact can be explained by taking into account that at temperatures lower than 450 °C the hydrotalcite undergoes the elimination of the interlayer water and the dehydroxylation process, without the collapse of the lamellar structure, but with a decreasing in the long-range ordering [30]. This process leads to a diminution of the basal spacing without generating the mesostructure of the MgAl mixed oxide. On the other hand, at temperatures higher than 450 °C the formation of $MgAl_2O_4$ spinel is favored. It has been already reported that the $MgAl_2O_4$ synthesised by means of coprecipitation method displays a lower S_{BET} and pore volume than the counterpart $MgAl(O)_x$ mixed oxide with periclase structure [44]. Moreover, it is observed a weight loss at temperatures higher than 450 °C which could be related to a decarbonation process of an amorphous $MgCO_3$ phase not detected by XRD, although its presence could be inferred from CO_2-TPD and FTIR techniques. Therefore, the pore structure of the mixed oxide generated from the thermal activation of hydrotalcite probably plays a fundamental role in both the glycerol conversion and the selectivity to DG.

The evolution of conversion and selectivity of the glycerol etherification with the reaction time (Fig. 9) reveals that, after an

Table 3
Influence of thermal treatment on the catalytic behaviour of MgAl_Na sample.

Temperature (°C)	Conversion (%)	Selectivity DG (%)	Selectivity TG (%)
n.a.[a]	32.8	100.0	0.0
200	31.6	100.0	0.0
450	50.7	84.8	15.2
650	31.4	94.8	5.2

[a] Non-activated sample.

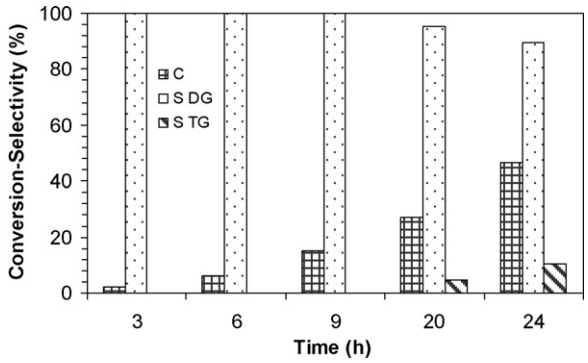

Fig. 9. Glycerol conversion and selectivities to DG and TG in the etherification reaction over the MgAl_Na catalyst versus time (same reactions conditions as Fig. 7).

induction period, the glycerol conversion is increased up to 47% after 24 h. However, within the first 3 h, 2.2% glycerol conversion is achieved. The only product detected at this low glycerol conversion was diglycerol. The presence of triglycerol is already detected for glycerol conversion higher than 27%, being the selectivity to triglycerol of 10% at 24 h. Although this catalyst is less active than homogeneous (Na_2CO_3) catalyst [24], the porous framework of MgAl mixed oxides clearly favours the formation of diglycerols.

Another key point in the use of solid catalysts in processes accomplished in liquid medium is the leaching of the active phase. It has been previously reported that catalysts based on La, Mg and Cs incorporated to mesoporous solids loss the active phase by leaching. In our case, the concentration of Mg and Al in the liquid phase is negligible, thus confirming the stability of these MgAl mixed oxides in the reaction medium.

4. Conclusions

A series of MgAl mixed oxides, obtained by calcination at 450 °C of hydrotalcites which have been synthesized by using two different precipitation methods (coprecipitation and urea hydrolysis), has been employed in the etherification of glycerol at 220 °C without solvent. These solids exhibit basic properties and excellent textural properties, making them suitable for base catalysed reaction, such as the etherification of glycerol. The highest conversion (50.7%) is found for the catalyst prepared by coprecipitation using $NaOH/Na_2CO_3$ as precipitating agent, with a maximum DG yield of 43%. However, full selectivity to diglycerols is only reached for low conversion values (14.6% for sample prepared by urea hydrolysis). Only DG and TG oligomers have been detected after 24 h of reaction. The formation of DG is favored at low conversion and in the presence of small pores.

Acknowledgements

The authors are grateful to the Spanish Ministry of Science and Innovation (ENE2009-12743-C04-03 project) and Junta de Andalucía (P09-FQM-5070) for financial support. RMT would like to thank this Ministry of Science and Innovation for the financial support under the Program Ramón y Cajal (RYC-2008-03387).

References

[1] C.H. Zhou, J.N. Beltramini, Y.X. Fan, G.Q. Lu, Chem. Soc. Rev. 37 (2008) 527–549.
[2] A. Behr, J. Eilting, K. Irawadi, J. Leschinski, F. Lindner, Green Chem. 10 (2008) 13–30.
[3] A. Brandner, K. Lehnert, A. Bienholz, M. Lucas, P. Claus, Top. Catal. 52 (2009) 278–287.
[4] T. Kurosaka, H. Maruyama, I. Naribayashi, Y. Sasaki, Catal. Commun. 9 (2008) 1360–1363.
[5] Z. Huang, F. Cui, H. Kang, J. Chen, C. Xia, Appl. Catal. A 366 (2009) 288–298.

[6] Y. Nakagawa, Y. Shinmi, S. Koso, K. Tomishige, J. Catal. 272 (2010) 191–194.
[7] D.A. Simonetti, J. Rass-Hansen, E.L. Kunkes, R.R. Soares, J.A. Dumesic, Green Chem. 9 (2007) 1073–1083.
[8] E.L. Kunkes, D.A. Simonetti, J.A. Dumesic, W.D. Pyrz, L.E. Murillo, J.G. Chen, D.J. Buttrey, J. Catal. 260 (2008) 164–177.
[9] K. Klepácová, D. Mravec, A. Kaszonyi, M. Bajus, Appl. Catal. A 328 (2007) 1–13.
[10] A.M. Ruppert, A.N. Parvulescu, M. Arias, P.J.C. Hausoul, P.C.A. Bruijnincx, R.J.M. Klein Gebbink, B.M. Weckhuysen, J. Catal. 268 (2009) 251–259.
[11] F. Frusteri, F. Arena, G. Bonura, C. Cannilla, L. Spadaro, O. Di Blasi, Appl. Catal. A 367 (2009) 77–83.
[12] J. Barrault, J.-M. Clacens, Y. Pouilloux, Top. Catal. 27 (2004) 137–142.
[13] M. Richter, Y.K. Krisnandi, R. Eckelt, A. Martin, Catal. Commun. 9 (2008) 2112–2116.
[14] A. Kraft, US Patent 6,649,690 (2003).
[15] R. Garcia, M. Besson, P. Gallezot, Appl. Catal. A 127 (1995) 165–176.
[16] W.C. Ketchie, M. Murayama, R.J. Davis, J. Catal. 250 (2007) 264–273.
[17] A. Corma, G.W. Huber, L. Sauvanaud, P. O'Connor, J. Catal. 257 (2008) 163–171.
[18] A. Ulgen, W. Hoelderich, Catal. Lett. 131 (2009) 122–128.
[19] Y.T. Kim, K.-D. Jung, E.D. Park, Microporous Mesoporous Mater. 131 (2010) 28–36.
[20] W. Yan, G.J. Suppes, Ind. Eng. Chem. Res. 48 (2009) 3279–3283.
[21] C. Márquez-Álvarez, E. Sastre, J. Pérez-Pariente, Top. Catal. 27 (2004) 105–117.
[22] A. Corma, S. Iborra, A. Velty, Chem. Rev. 107 (2007) 2411–2502.
[23] J.M. Clacens, Y. Pouilloux, J. Barrault, C. Linares, M. Goldwasser, Stud. Surf. Sci. Catal. 118 (1998) 895.
[24] J.M. Clacens, Y. Pouilloux, J. Barrault, Appl. Catal. A 227 (2002) 181–190.
[25] J.M. Clacens, Y. Pouilloux, J. Barrault, Surf. Sci. Catal. 143 (2002) 687–695.
[26] A.M. Ruppert, J.D. Meeldijk, B.W.M. Kuipers, B.H. Erné, B.M. Weckhuysen, Chem. Eur. J. 14 (2008) 2016–2024.
[27] F. Cavani, F. Trifiró, A. Vaccari, Catal. Today 11 (1991) 173–301.
[28] A. Corma, S. Iborra, S. Miquel, J. Primo, J. Catal. 173 (1998) 315–321.
[29] D. Tichit, B. Coq, Catal. Technol. 7 (2003) 206–217.
[30] J. Pérez-Ramírez, S. Abelló, N.M. van der Pers, Chem. Eur. J. 13 (2007) 870–878.
[31] A. Corma, S. Iborra, S. Miquel, WO9856747 (1998).
[32] M. Di Serio, M. Ledda, M. Cozzolino, G. Minutillo, R. Tesser, E. Santacesaria, Ind. Eng. Chem. Res. 45 (2006) 3009–3014.
[33] Y. Liu, E. Lotero, J.G. Goodwin, X. Mo, Appl. Catal. A 331 (2007) 138–148.
[34] M.C.G. Albuquerque, J. Santamaría-González, J.M. Mérida-Robles, R. Moreno-Tost, E. Rodríguez-Castellón, A. Jiménez-López, D.C.S. Azevedo, C.L. Cavalcante Jr., P. Maireles-Torres, Appl. Catal. A 347 (2008) 162–168.
[35] M.A. Aramendía, Y. Avilés, J.A. Benítez, V. Borau, C. Jiménez, J.M. Marinas, J.R. Ruiz, F.J. Urbano, Microporous Mesoporous Mater. 29 (1999) 319–328.
[36] C. Noda Pérez, C.A. Pérez, C.A. Henriques, J.L.F. Monteiro, Appl. Catal. A 272 (2004) 229–240.
[37] M. Adachi-Pagano, C. Forano, J.P. Besse, J. Mater. Chem. 13 (2003) 1988–1993.
[38] I. Pausch, H.H. Lohse, K. Schürmann, R. Allmann, Clays Clay Miner. 24 (1986) 507–510.
[39] S. Abelló, J. Pérez-Ramírez, Microporous Mesoporous Mater. 96 (2006) 102–108.
[40] E. Angelescu, O.D. Pavel, R. Bîrjega, M. Florea, R. Zavoianu, Appl. Catal. A 341 (2008) 50–57.
[41] M.J. Climent, A. Corma, S. Iborra, J. Primo, J. Catal. 151 (1995) 60–66.
[42] D. Tichit, M.H. Lhouty, A. Guida, B.H. Chiche, F. Figueras, A. Auroux, D. Bartalini, E. Garrone, J. Catal. 151 (1995) 50–59.
[43] B.F. Sels, D.E. De Vos, P.A. Jacobs, Catal. Rev. 43 (2001) 443–488.
[44] S. Bocanegra, A.D. Ballarini, O.A. Scelza, S.R. de Miguel, Mater. Chem. Phys. 111 (2008) 534–541.